Optics Measurements, Corrections and Modelling for High-Performance Storage Rings workshop (OMCM)

The DAΦNE experience

Catia Milardi

June 20th ÷ 22nd 2011, CERN, Geneva

Outline

- *DAΦNE Main Rings*
- *Beam Position diagnostics*
- *Optics Measurements*
- *Closed Orbit steering and correction*
- σ_y *tuning and control*
- *Betatron Coupling analysis and minimization*

Main Rings magnetic layout

General aspects:

- Double ring collider
- Compact magnetic layout
- No periodicity
- All magnetic elements are independently powered
- 4 wigglers in each ring
- 8 dipoles, 4 different kinds each ring, not negligible fringing fields
- Cross talk between e+ and e- ring
- Cross talk between e- transfer lines and ring
- Off axis orbit in the low-beta quadrupoles due to horizontal crossing angle at the IP
- Detector solenoidal field (KLOE and FINUDA) strongly affecting ring optics

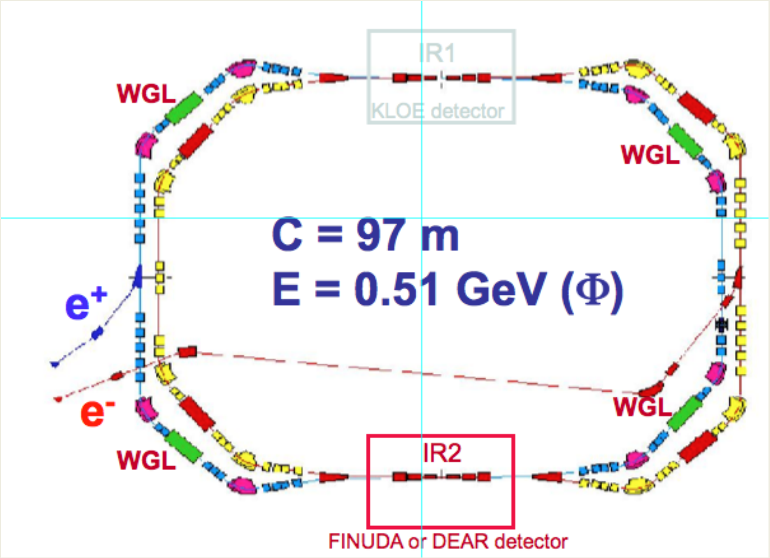

2001 ÷ 2007

Two 10 meter long IRs common to the colliding beams

Non-linear terms in the wiggler field almost halved

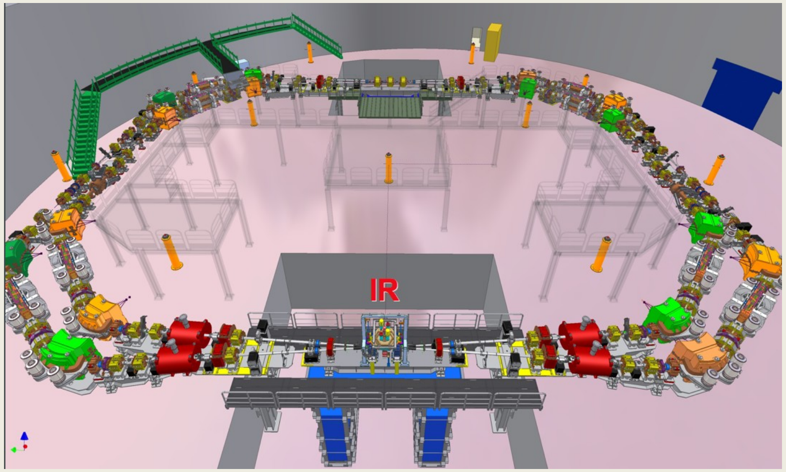

2007 ÷ 2011

One IR and complete beam separation 50 cm apart from the IP

Crab-Waist collision scheme

DAΦNE BPMs

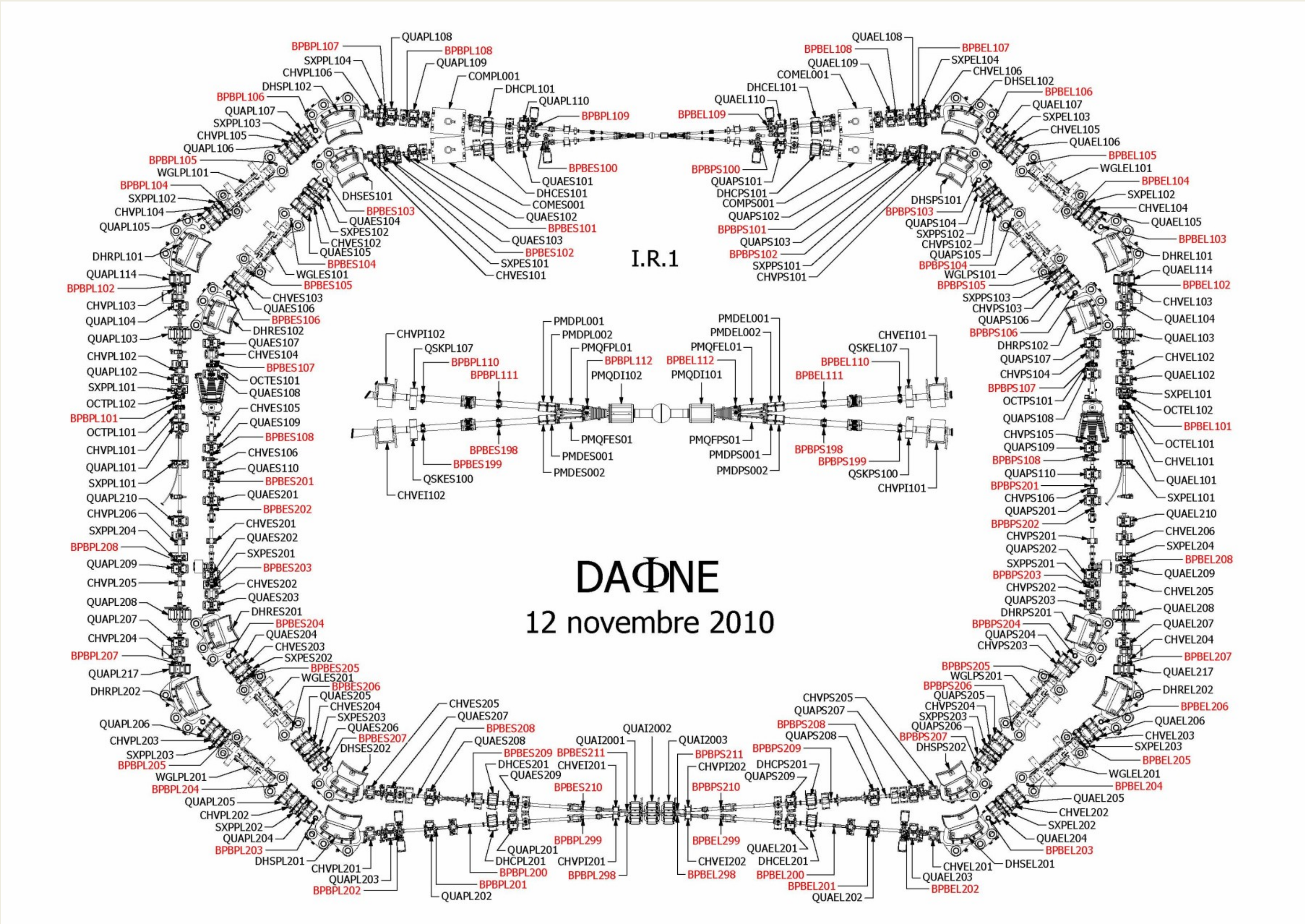

I.R.1
DAΦNE
12 novembre 2010
QUAPL108
BPBPL107
BPBPL108
SXPPL104
QUAPL109
CHVPL106
COMPL001
DHSPL102
DHCPL101
BPBPL106
QUAPL110
QUAPL107
BPBPL109
SXPPL103
CHVPL105
QUAPL106
BPBPL105
WGLPL101
BPBPL104
SXPPL102
CHVPL104
QUAPL105
DHRPL101
QUAPL114
BPBPL102
CHVPL103
QUAPL104
QUAPL103
CHVPL102
QUAPL102
SXPPL101
OCTPL102
BPBPL101
OCTPL101
CHVPL101
QUAPL101
SXPPL101
QUAPL210
CHVPL206
SXPPL204
BPBPL208
QUAPL209
CHVPL205
QUAPL208
QUAPL207
CHVPL204
BPBPL207
QUAPL217
DHRPL202
QUAPL206
CHVPL203
SXPPL203
BPBPL205
WGLPL201
BPBPL204
QUAPL205
CHVPL202
SXPPL202
QUAPL204
BPBPL203
DHSPL201
CHVPL201
QUAPL203
BPBPL202
QUAPL202
BPBES100
QUAES101
DHCES101
COMES001
QUAES102
BPBES101
QUAES103
BPBES102
SXPES101
CHVES101
DHSES101
BPBES103
QUAES104
SXPES102
CHVES102
QUAES105
BPBES104
WGLES101
BPBES105
CHVES103
QUAES106
BPBES106
DHRES102
QUAES107
CHVES104
BPBES107
OCTES101
QUAES108
CHVES105
QUAES109
BPBES108
CHVES106
QUAES110
BPBES201
QUAES201
BPBES202
CHVES201
QUAES202
SXPES201
BPBES203
CHVES202
QUAES203
DHRES201
BPBES204
QUAES204
CHVES203
SXPES202
BPBES205
WGLES201
BPBES206
QUAES205
CHVES204
SXPES203
QUAES206
BPBES207
DHSES202
CHVES205
QUAES207
BPBES208
QUAES208
BPBES209
DHCES201
QUAES209
BPBES210
QUAPL201
DHCPL201
BPBPL200
BPBPL201
CHVPI201
BPBPL298
BPBPL299
QUAI2001
BPBES211
CHVEI201
QUAI2002
QUAI2003
BPBPS211
CHVPI202
BPBPS210
BPBEL299
CHVEI202
BPBEL298
QUAEL201
DHCEL201
BPBEL200
BPBEL201
QUAEL202
DHCPS201
QUAPS209
BPBPS209
QUAPS208
BPBPS208
QUAPS207
CHVPS205
CHVPI102
QSKPL107
BPBPL110
BPBPL111
PMDPL001
PMDPL002
PMQFPL01
BPBPL112
PMQDI102
PMQFES01
PMDES001
PMDES002
BPBES198
BPBES199
QSKES100
CHVEI102
PMDEL001
PMDEL002
PMQFEL01
BPBEL112
PMQDI101
BPBEL110
BPBEL111
QSKEL107
CHVEI101
PMQFPS01
PMDPS001
PMDPS002
BPBPS198
BPBPS199
QSKPS100
CHVPI101
QUAEL108
BPBEL108
BPBEL107
QUAEL109
SXPEL104
COMEL001
CHVEL106
DHCEL101
DHSEL102
QUAEL110
BPBEL106
BPBEL109
QUAEL107
SXPEL103
CHVEL105
QUAEL106
BPBEL105
WGLEL101
BPBEL104
SXPEL102
CHVEL104
QUAEL105
BPBEL103
DHREL101
QUAEL114
BPBEL102
CHVEL103
QUAEL104
QUAEL103
CHVEL102
QUAEL102
SXPEL101
OCTEL102
BPBEL101
OCTEL101
CHVEL101
QUAEL101
SXPEL101
QUAEL210
CHVEL206
SXPEL204
BPBEL208
QUAEL209
CHVEL205
QUAEL208
QUAEL207
CHVEL204
BPBEL207
QUAEL217
DHREL202
BPBEL206
QUAEL206
CHVEL203
SXPEL203
BPBEL205
WGLEL201
BPBEL204
QUAEL205
CHVEL202
SXPEL202
QUAEL204
BPBEL203
CHVEL201
DHSEL201
QUAEL203
BPBEL202
BPBPS100
QUAPS101
DHCPS101
COMPS001
QUAPS102
BPBPS101
QUAPS103
BPBPS102
SXPPS101
CHVPS101
DHSPS101
BPBPS103
QUAPS104
SXPPS102
CHVPS102
QUAPS105
BPBPS104
WGLPS101
BPBPS105
SXPPS103
CHVPS103
QUAPS106
BPBPS106
DHRPS102
QUAPS107
CHVPS104
BPBPS107
OCTPS101
QUAPS108
CHVPS105
QUAPS109
BPBPS108
QUAPS110
BPBPS201
CHVPS106
QUAPS201
BPBPS202
CHVPS201
QUAPS202
SXPPS201
BPBPS203
CHVPS202
QUAPS203
DHRPS201
BPBPS204
QUAPS204
CHVPS203
BPBPS205
WGLPS201
BPBPS206
QUAPS205
CHVPS204
SXPPS203
QUAPS206
BPBPS207
DHSPS202

BPM acquisition system

- 120 pickups
- 4 parallel CPUs

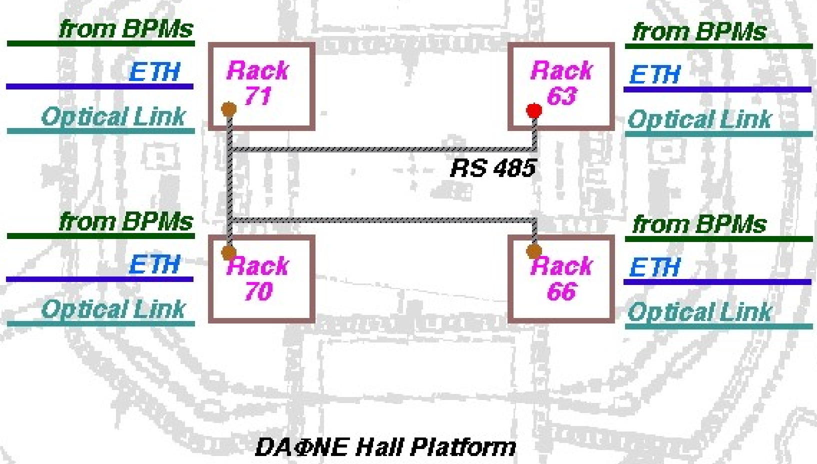

Pickup details:
Button electrodes 10 mm diameter
50 Ω matched impedance
4.2 pF capacitance

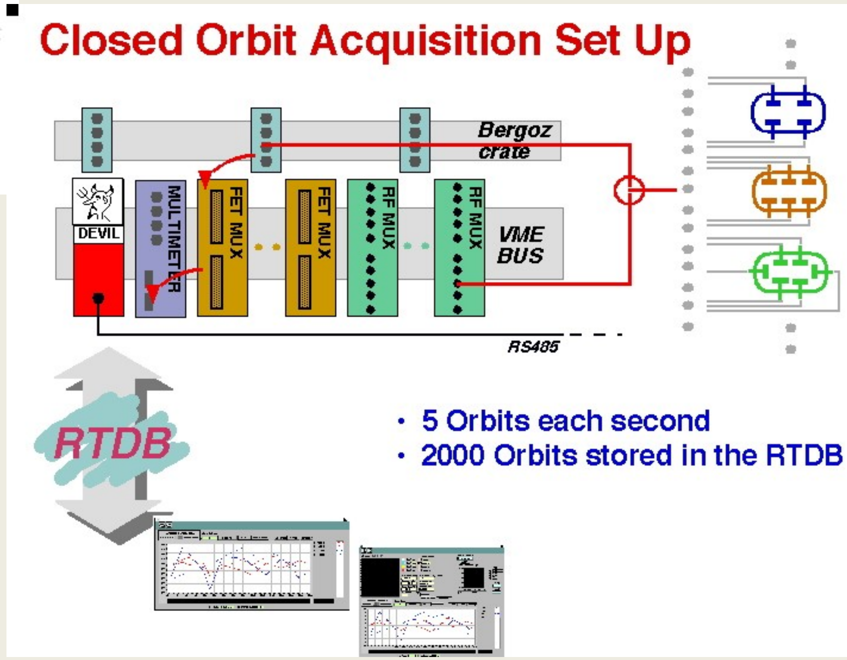

BPM transfer function obtained by:
Numerical simulation
Bench measurement
then used to compensate pickup nonlinearities in the range +/- 20 mm

In 2006 4 additional BPMs acquisition systems based on LIBERA modules have been added on each ring

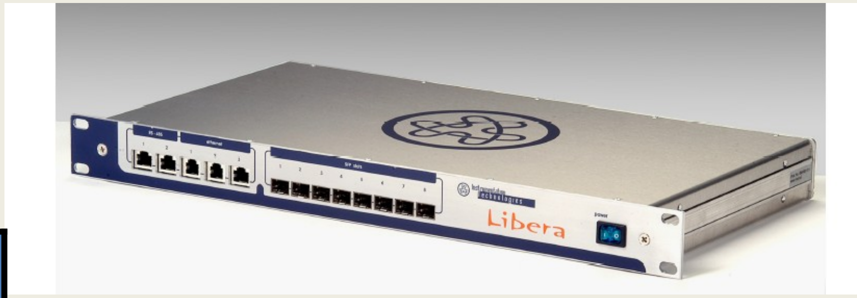

recovery after a major Shutdown	Not yet stored beam •Trajectory •Central rev frequency •Tune	Not available in present system
machine studies	Turn by turn (non linear terms)	Dedicated tracking system
	√Beta phase advance	Dedicated system
normal operation	Closed orbit	Improved resolution
	Tune	Dedicated system

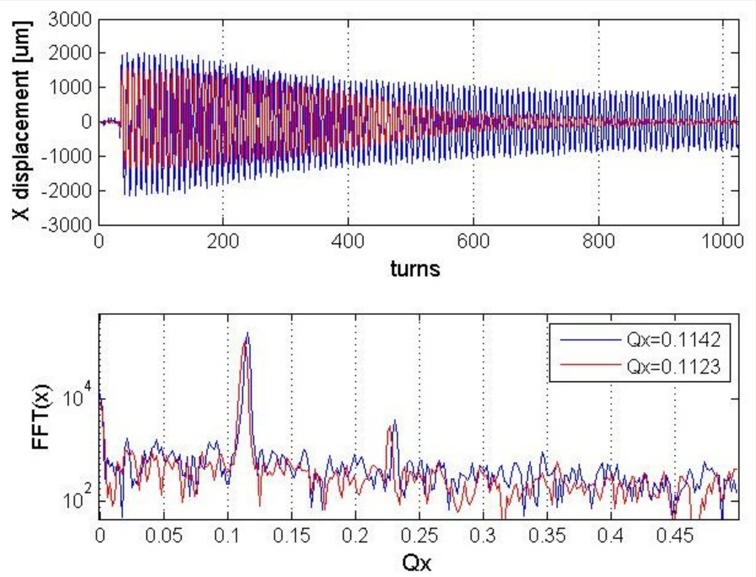

BPM resolution versus beam current

each point is averaged on 100 orbit

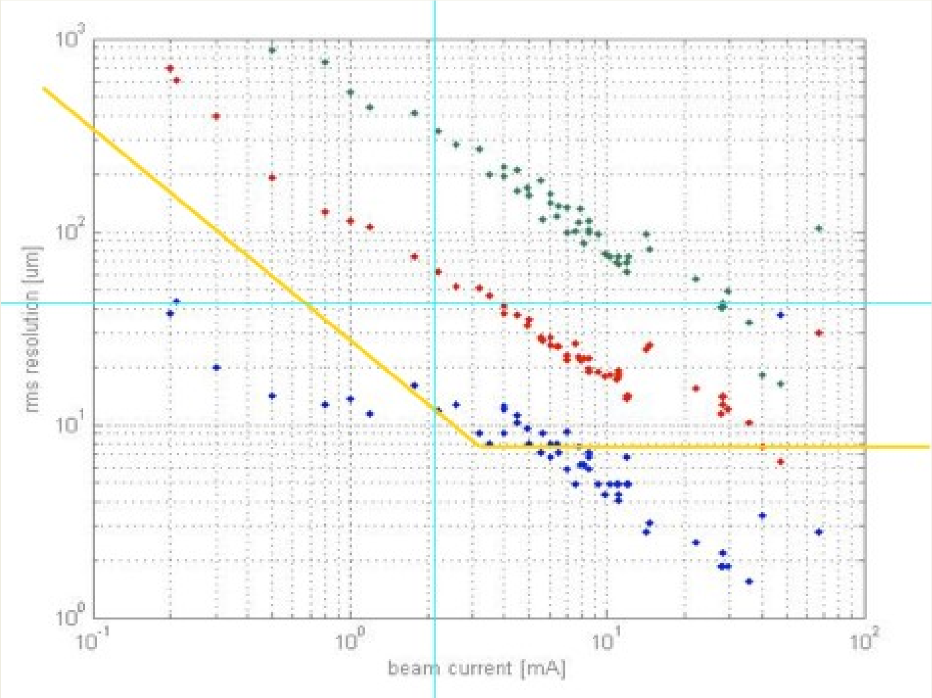

----: Bergoz system resolution
♦: libera slow acquisition mode
♦: Libera turn by turn mode
♦: Libera turn by turn mode (decimated)

For the Bergoz system:

$\delta x \sim 0.01$ mm above $\langle I \rangle_{treshold}$

$\langle I \rangle_{treshold}$ =

3.1 mA (round, diagonal, rect, wiggler)

2.1 mA (dipole, interaction region)

Measured Response Matrix

From Correctors

- orbit correction
- closed bump calculation
- corrector strength reduction
- understand & improve machine linear-model
- dispersion function control
- coupling evaluation

From Quadrupoles

- beam based alignment

i=1..n_c n_c = 29 for CHV n_C = 51 for QUADs
j=1..n_{mon} n_{mon} = 44

$$z_i = \frac{\sqrt{\beta_i \beta_j}}{2\sin(\pi\nu)} \cos \nu(|\phi_i - \phi_j| - \pi)$$

z = x,y

$$A_{ij} = \frac{\partial z_j}{\partial \vartheta_i} \qquad \vartheta_i[mrad] = C_i \frac{I_i[A]}{E[MeV]}$$

$$A_{ij} = \frac{\partial z_j}{\partial I_i}$$

$$A^H = \begin{vmatrix} A^{HH} & 0 \\ 0 & A^{HV} \end{vmatrix}$$

$$A^V = \begin{vmatrix} 0 & A^{VV} \\ A^{VH} & 0 \end{vmatrix}$$

Closed Orbit correction & Beam Steering by measured Response Matrix

- Global Orbit Correction

$$\bar{z} = A \Delta \bar{I}$$

- Corrector strength reduction

$$(\bar{z} + A\bar{I}_0) = A\bar{I}$$

Equations are least square solved by Singular Value Decomposition

- Best Corrector useful in identifying power supply faults & drifts

$$I_j = \frac{\sum_i z_i A_{ij}}{\sum_i A_{ij}^2}$$

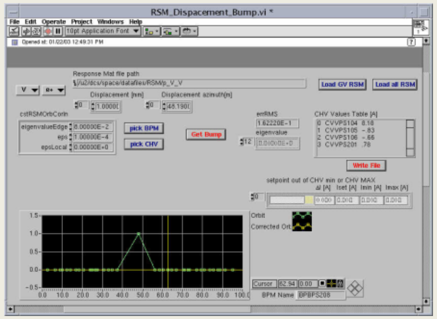

These algorithms are unaffected from:

- model imperfection
- corrector calibration constant
- offset in BPMs alignment
- overall offset in orbit readout

Best Orbit at DAΦNE

Closed Orbit Correction and steering magnet strength minimization to:

- Point out errors in the magnetic layout
- Reduce non-linear contributions to the beam optics (ε_x, α_c, τ)
- Keep beam dispersion under control
- Minimize transverse coupling (ε_y, κ)
- reduce background hitting the experimental detector and ameliorate scrapers efficiency

Orbit can be made as small as desired, however the most suitable value for operation is obtained iteratively by global, local correction and steering magnet strength minimization.

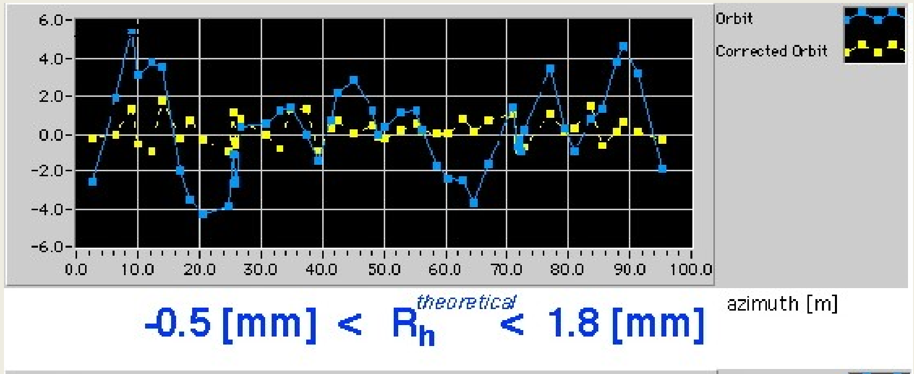

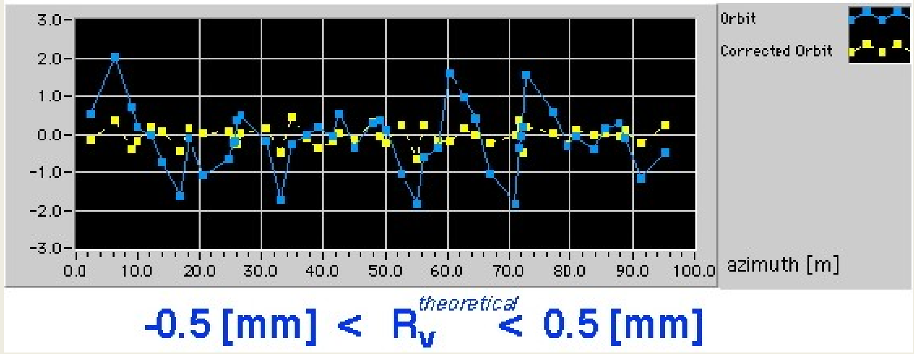

Bare orbit minimization by element alignment

$$z_{bare} = z_{beam} - z_{\sum Steers}$$

- A large bare orbit indicates always alignment problems
- Misalignment errors are identified by fitting the measured bare orbit with the machine model

In the example:

Bare orbit has been reduced in both rings by repositioning the outer electromagnetic QUADS in the FINUDA IR

After alignment:

- strengths of the steering magnets adjacent to the IR2 section are considerably reduced
- bare orbit is significantly reduced and is comparable in the two rings

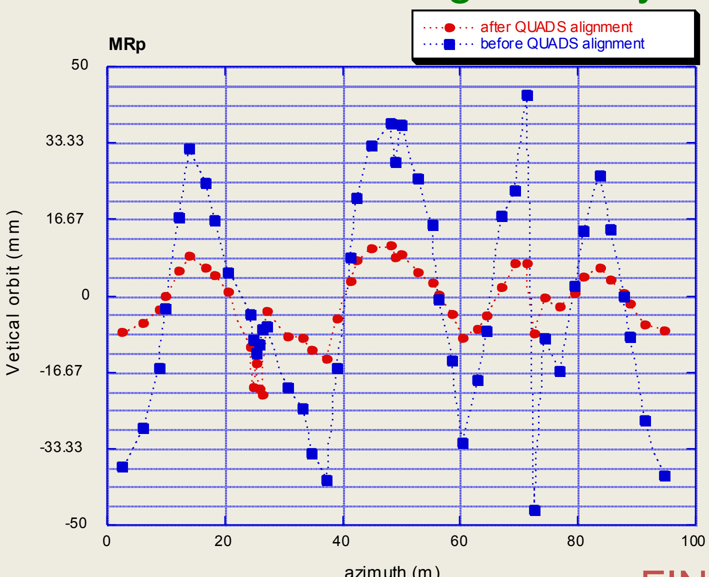

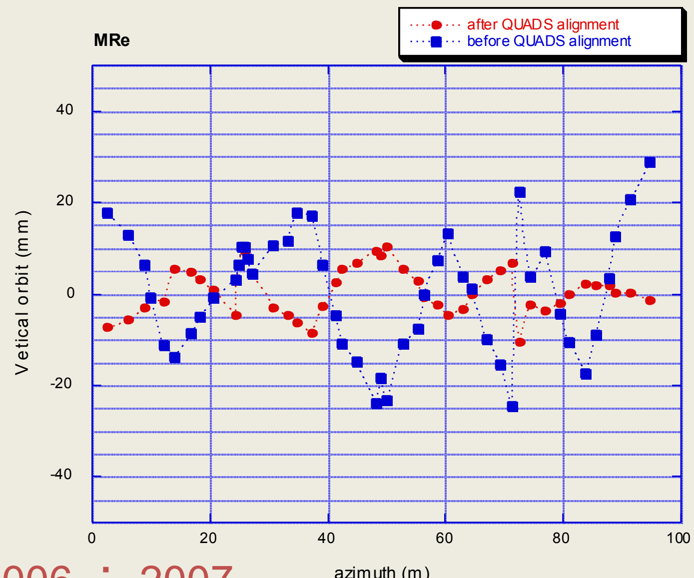

FINUDA run 2006 ÷ 2007

Twiss function measurement & ring optics

β measurements performed by:

- varying the quadrupole strength (**42 QUADs per ring**)
- Correcting the closed orbit variation, if any
- the β value precision depends on the accuracy of the tune measurement, possible systematic errors in the quadrupoles calibration are neglected

Optics measurements (β_1, β_2, ν_1, ν_2, η_x, η_x, ξ_x, ξ_y) are used for model optimization

The model is used for:

- optics computation
- measurements analysis
- lifetime computation
- dynamic aperture studies
- background, beam-beam and e-cloud simulations

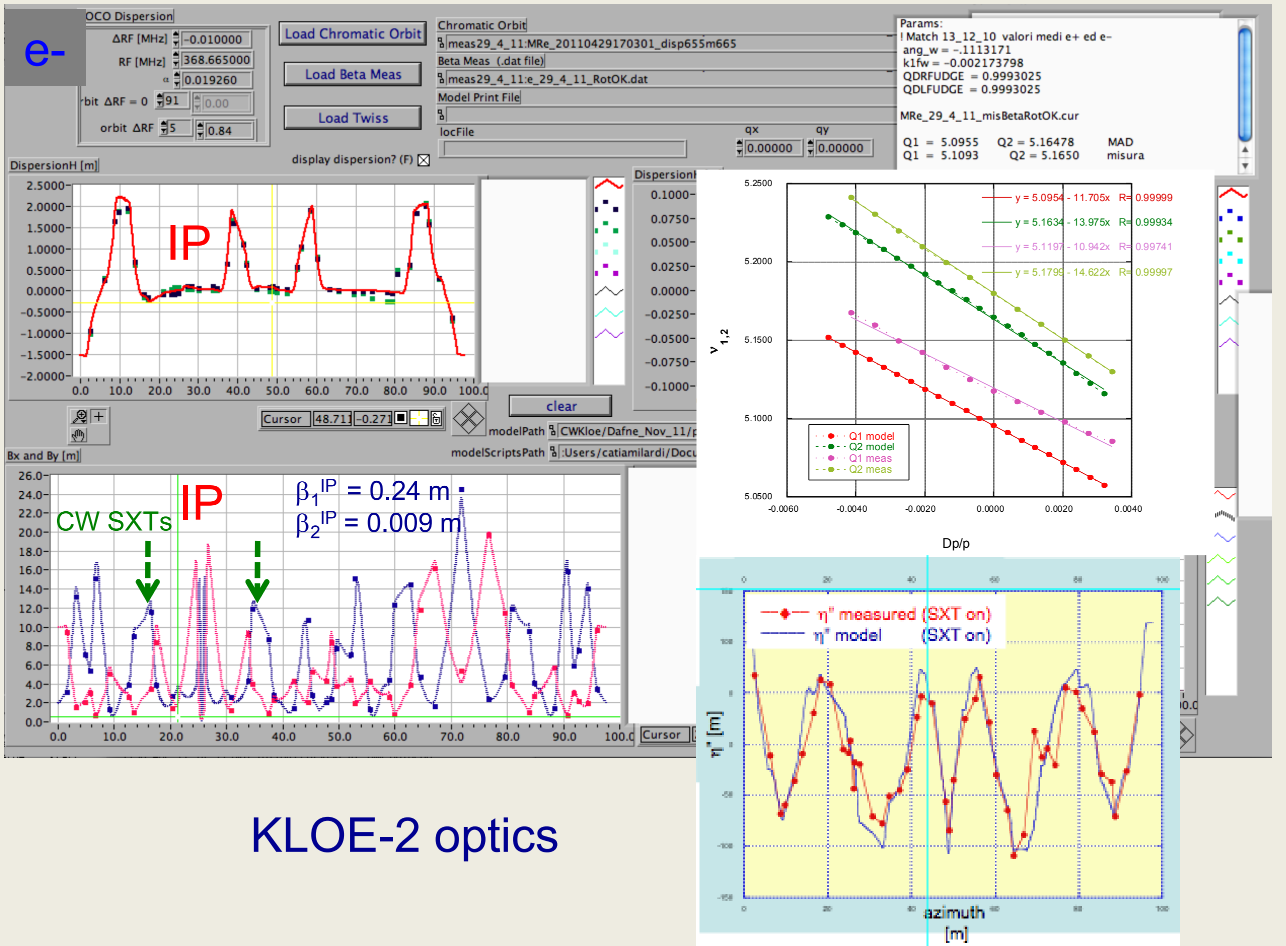

KLOE-2 optics

β-function evaluation by measured Response Matrix

$$R_{ij} = \frac{\sqrt{\beta_i \beta_j}}{2\sin(\pi\nu)} \cos \nu(|\phi_i - \phi_j| - \pi)$$

$i=1 \ldots n_{BPM} = 44$

$j=1 \ldots n_{CHV} = 29$

$n_{BPM} + n_{CHV} = 73$

- **β** can be evaluated in automatic and fast way at all BPMs and CHVs
- The equation system given by the R matrix is solved iteratively by using SVD numerical technique
- The procedure starts from an initial set of (β_i ϕ_i) and (β_j ϕ_j) and stops when ν converges to the measured value
- Ambiguity in the β determination can be avoided by imposing equal β at a couple of adjacent BPM and CHV

β_x compared with the MAD model (e^- ring)

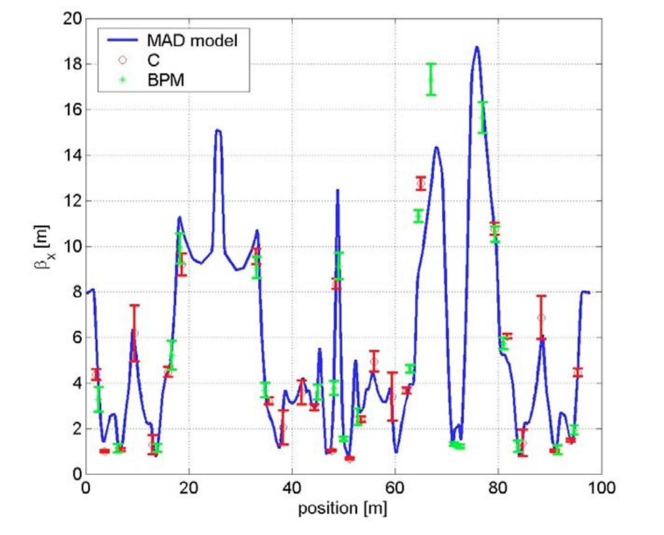

β_y compared with the MAD model (e^- ring)

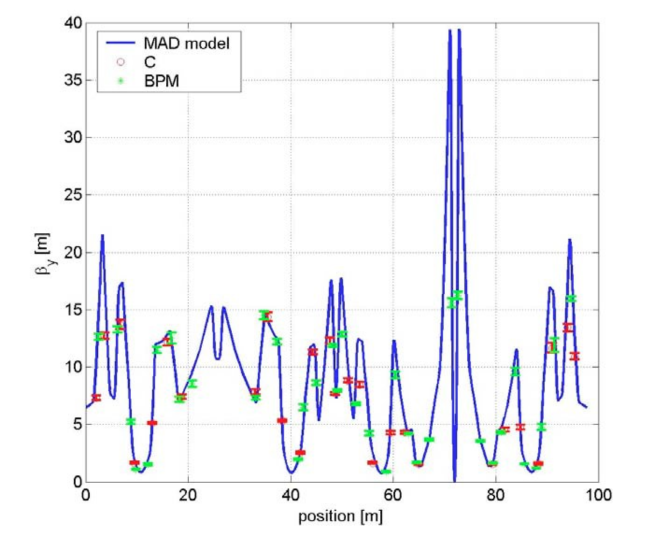

DEAR run (2002)

Original DEAR IR:

IR^{DEAR} (Q_F Q_D Q_F) $\beta^*_x = 4.4$ m $\beta^*_y = 0.04$ m

New DEAR low-beta

IR^{DEAR} (Q_D Q_F)

$\beta^*_x = 1.7$ [m] $\beta^*_y = 0.03$ [m]

$\alpha^*_x = 25 \rightarrow 29$ mrd

β^{PC}_x reduced by 50%

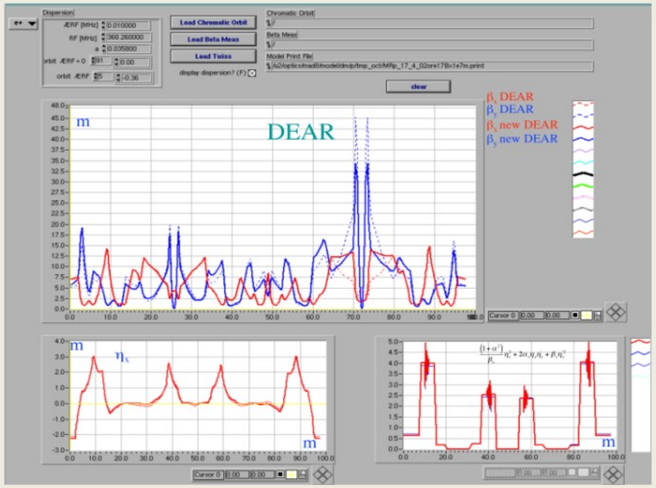

100 contiguous bunches in collision for the first time

!

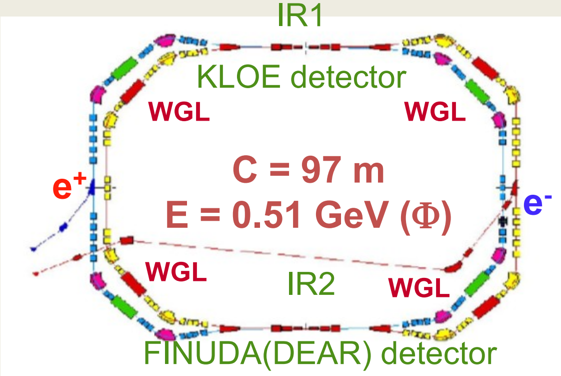

The KLOE IR is going to be modified according the DEAR one

Parasitic Crossings in the DAFNE IR1 (KLOE run 2005)

In the original DAFNE IRs the beams experienced 24 Long Range Beam Beam interactions

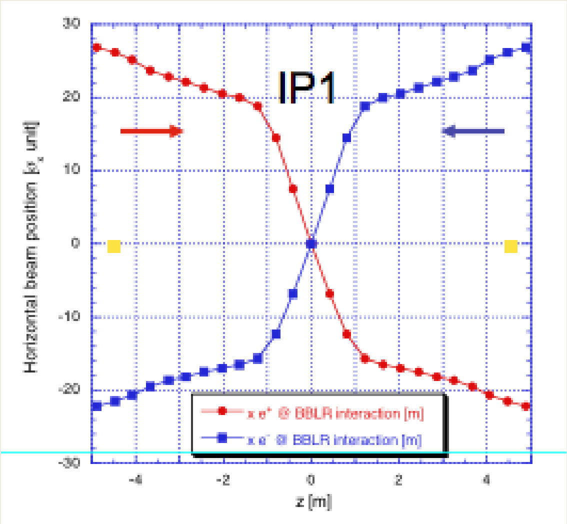

computed orbit deflection due to 24 LRBB interactions for the positron bunch colliding against 10 mA electron bunches.

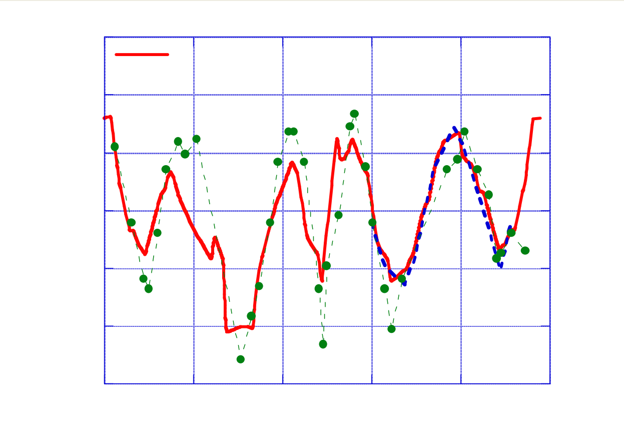

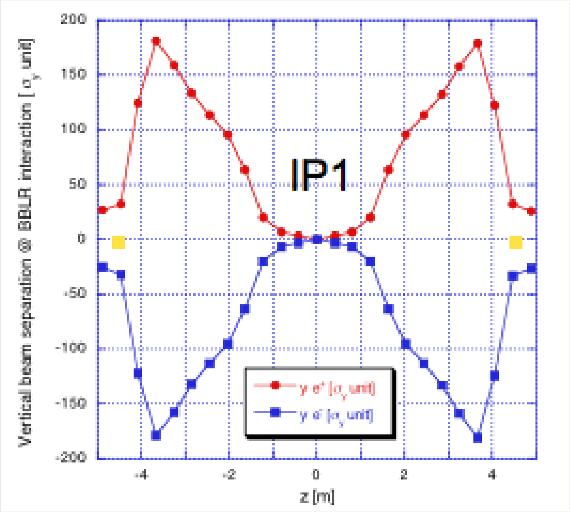

LIFETRACK simulation

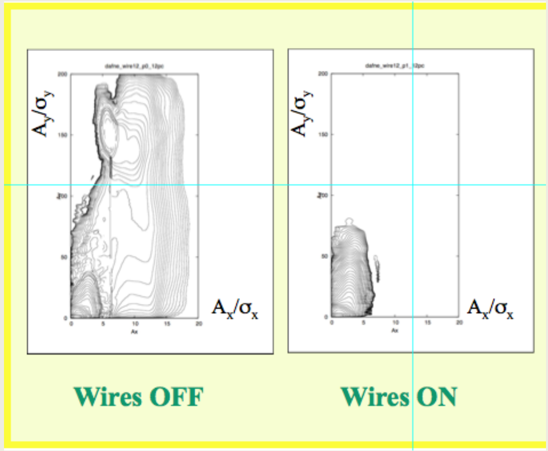

- 2 current currying windings (wires) installed at both ends of the KLOE interaction region (IR)
- It's necessary to separate the beams as close as possible after the IP

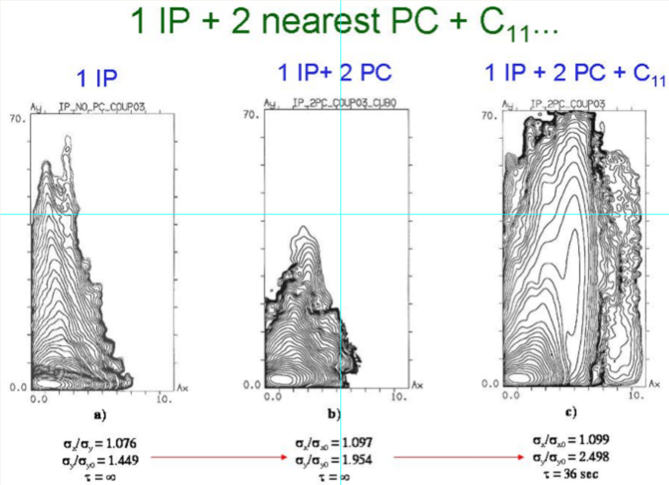

Working point & nonlinearities compensation tuning during II FINUDA run (Nov 06 ÷ May 07)

$\nu^-_x = 086 \quad \nu^+_x = .1090$

$\nu^-_y = .1560 \quad n^+_y = .1910.$

$\nu^-_x = .076 \quad \nu^+_x = .096$

$\nu^-_y = .14 \quad \nu^+_y = .168$

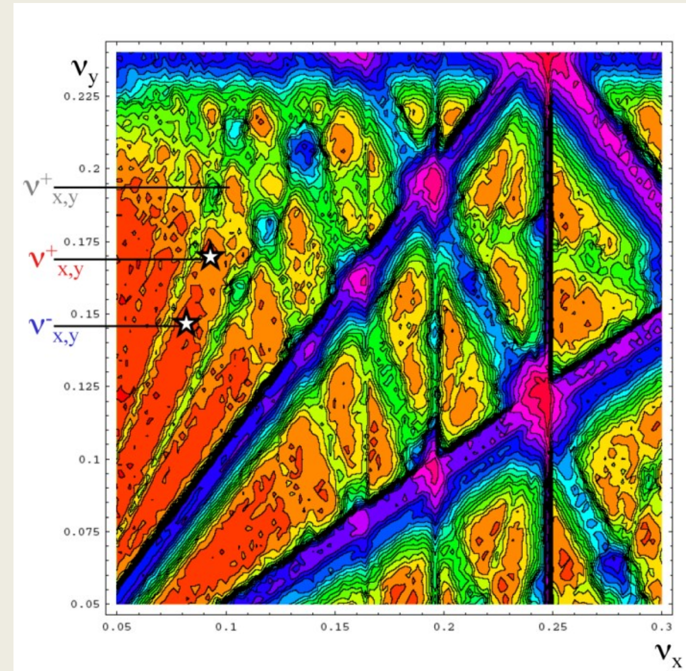

- Improve peak luminosity
- limit beam-beam blow-up at high currents

During e^- beam injection

$\Delta\nu^+_{x,y} = 0.0005 \div 0.0015$

$\Delta k^+_3 = 5. \div 15$ A

double the e+ beam llifetime

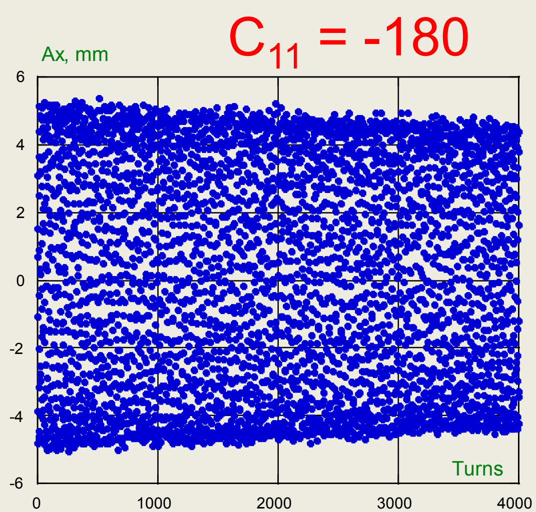

Octupole ON (I =43 A)

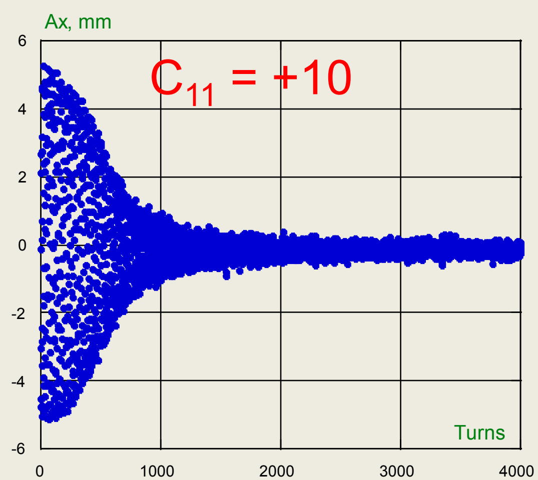

Octupole OFF

Octupole variation affects:

- c_{11}
- dynamic aperture
- ξ”

DAΦNE optics with negative momentum compaction

(KLOE run 2004÷2006)

- Bunch lengthening with current is considerably reduced
- Head-tail instability occurs for $\xi_{x,y} > 0$, the ring can be operated without or with very weak sextupoles
- Beam-beam is in general less harmful and the beam is in general more stable

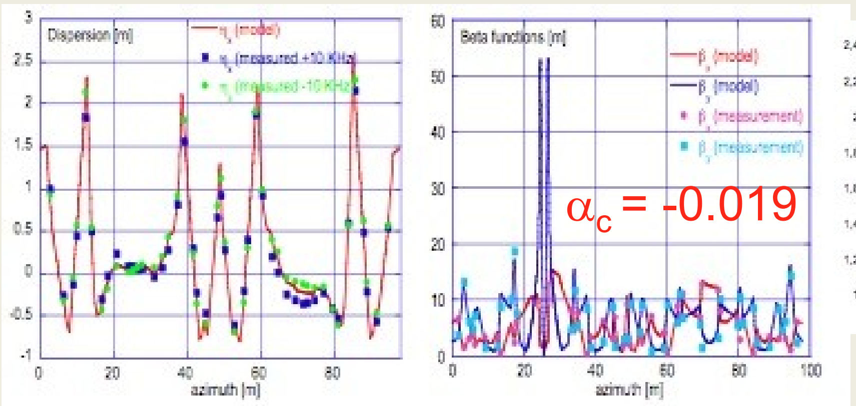

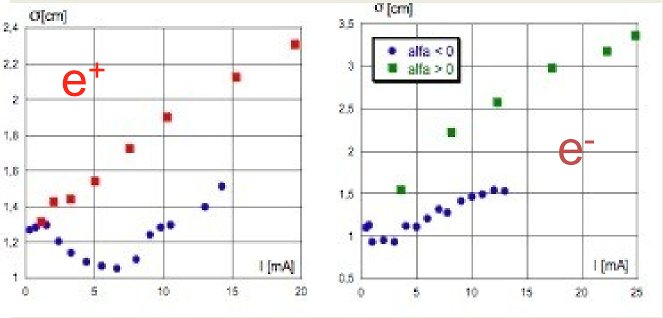

Collision $\alpha_c < 0$

- $L_{peak} \sim 2.5 \cdot 10^{31}$ $cm^{-2}\ s^{-1}$
- $I^- \sim 0.3$ A $n_b = 100$
- $I^+ \sim 0.3$ A

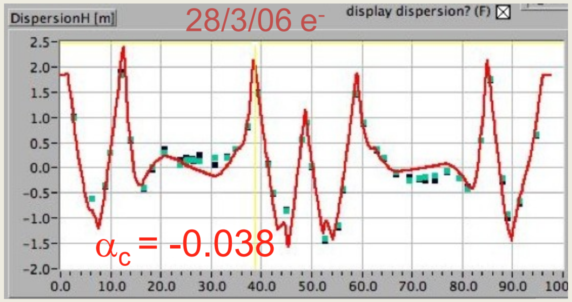

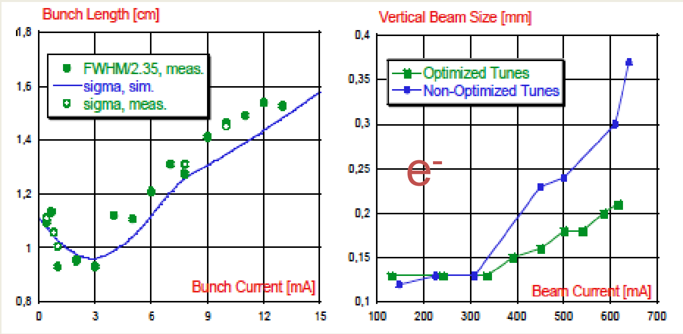

A strong correlation has been observed between the longitudinal microwave instability and the vertical size blow-up

e- Vertical Size Blow-up with large α_c

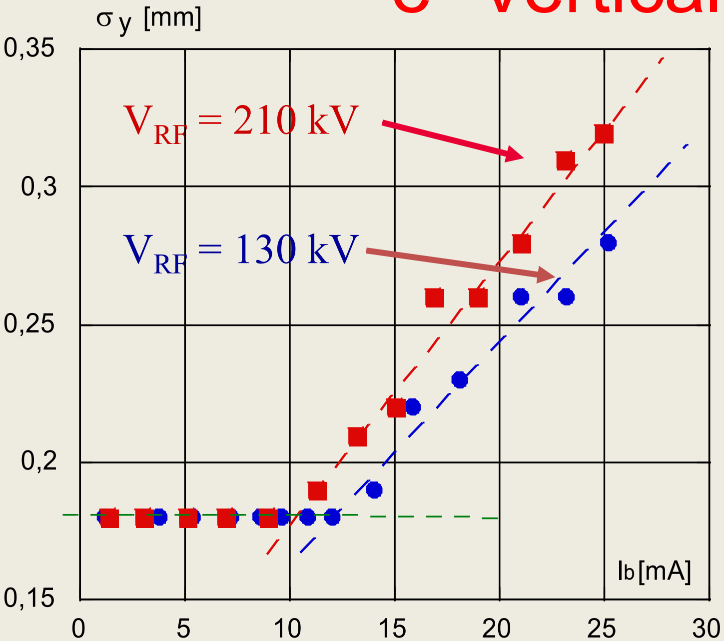

Data from KLOE run Apr. 05

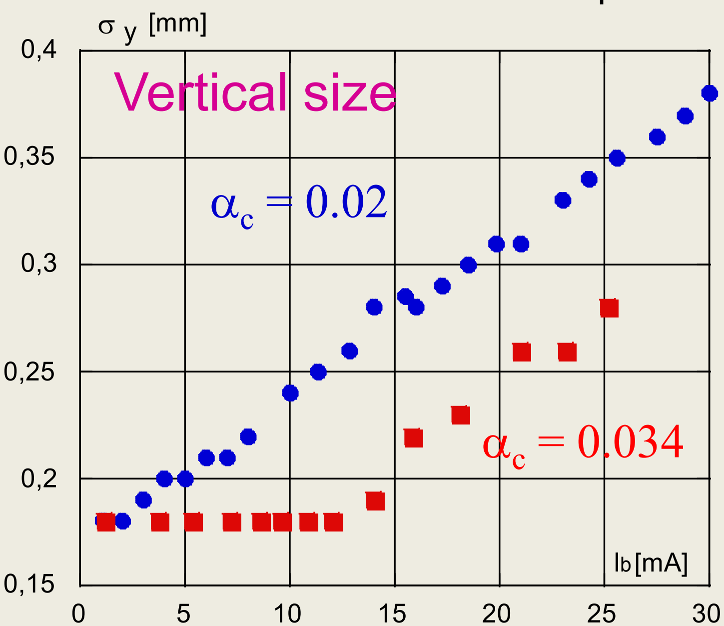

- Single bunch (beam) effect
- It is correlated with the longitudinal microwave instability treshold:

$$Threshold \quad scales \approx \sqrt{\frac{1}{V_{RF}}} \propto 1.27$$

- It is relevant for the e- ring having higher coupling impedance

- The threshold is higher for higher momentum compaction

It is necessary to reduce the ring impedance

σ_y tuning

High luminosity cannot be achieved without a careful control of the σ_y parameter

$$\sigma_y = \sqrt{\varepsilon_y \beta_y + \eta_y^2 \sigma_p^2} \qquad \varepsilon_y = \varepsilon_0 \frac{\kappa}{1+\kappa}$$

Dominant source of σ_y are:

- large vertical orbit
- vertical dispersion
- transverse betatron coupling due to:
  - experimental solenoid
  - roll errors in quadrupoles
  - vertical orbit distortion in sextupoles
- vacuum chamber impedance

Vertical Dispersion minimization

Correcting orbit and dispersion at the same time by using orbit and dispersion dependence on the **steering magnets** and on the **skew quadrupoles** current

$$\overline{y} = K \Delta \overline{I}_s$$

BPM *i=1 ... n_m = 44*
Corrector *j=1 ... n_C = 29*
Skew Quadrupole *N_s = 10*

$$y = \begin{pmatrix} \frac{\partial y_1}{\partial C_{h1}} \\ . \\ \frac{\partial y_{Nm}}{\partial C_{h1}} \\ . \\ . \\ . \\ \frac{\partial y_1}{\partial C_{hNc}} \\ . \\ \frac{\partial y_{Nm}}{\partial C_{hNc}} \\ \frac{\partial y_1}{\partial f_{RF}} \\ . \\ \frac{\partial y_{Nm}}{\partial f_{RF}} \end{pmatrix}$$

Ns

$(N_m * N_c) + N_m$

$$K = \begin{pmatrix} \frac{\partial y_1}{\partial C_{h1} \partial S_1} \mathrm{K\ K} \frac{\partial y_1}{\partial C_{h1} \partial S_{Ns}} \\ \mathrm{K\ K\ K\ K\ K\ K\ K\ K\ K} \\ \frac{\partial y_{Nm}}{\partial C_{h1} \partial S_1} \mathrm{K\ K} \frac{\partial y_{Nm}}{\partial C_{h1} \partial S_{Ns}} \\ \mathrm{K\ K\ K\ K\ K\ K\ K\ K\ K} \\ \mathrm{K\ K\ K\ K\ K\ K\ K\ K\ K} \\ \mathrm{K\ K\ K\ K\ K\ K\ K\ K\ K} \\ \frac{\partial y_1}{\partial C_{hNc} \partial S_1} \mathrm{K\ K} \frac{\partial y_1}{\partial C_{hNc} \partial S_{Ns}} \\ \mathrm{K\ K\ K\ K\ K\ K\ K\ K\ K} \\ \frac{\partial y_{Nm}}{\partial C_{hNc} \partial S_1} \mathrm{K\ K} \frac{\partial y_{Nm}}{\partial C_{hNc} \partial S_{Ns}} \\ \frac{\partial y_1}{\partial f_{RF} \partial S_1} \mathrm{K\ K} \frac{\partial y_{Nm}}{\partial f_{RF} \partial S_{Ns}} \\ \mathrm{K\ K\ K\ K\ K\ K\ K\ K\ K} \\ \frac{\partial y_{Nm}}{\partial f_{RF} \partial S_1} \mathrm{K\ K} \frac{\partial y_{Nm}}{\partial f_{RF} \partial S_{Ns}} \end{pmatrix}$$

Vertical Dispersion minimization

Correcting orbit and dispersion at the same time using orbit and dispersion dependence on the steering magnets

$$\bar{u} = D \Delta \bar{I}$$

i=1 … $n_{mon} = 44$

j=1 … $n_{CHV} = 29$

$$u = \begin{vmatrix} y_1 \\ . \\ y_{n_{mon}} \\ \eta_1 \\ . \\ \eta_{n_{mon}} \end{vmatrix} \quad 2{*}n_{mon}$$

$$D = \begin{vmatrix} . & . & . & . & . \\ . & . & \dfrac{\partial y_i}{\partial I_j} & . & . \\ . & . & . & . & . \\ . & . & . & . & . \\ . & . & \dfrac{\partial \eta_i}{\partial I_j} & . & . \\ . & . & . & . & . \end{vmatrix} \quad 2{*}n_{mon} \times n_{kick}$$

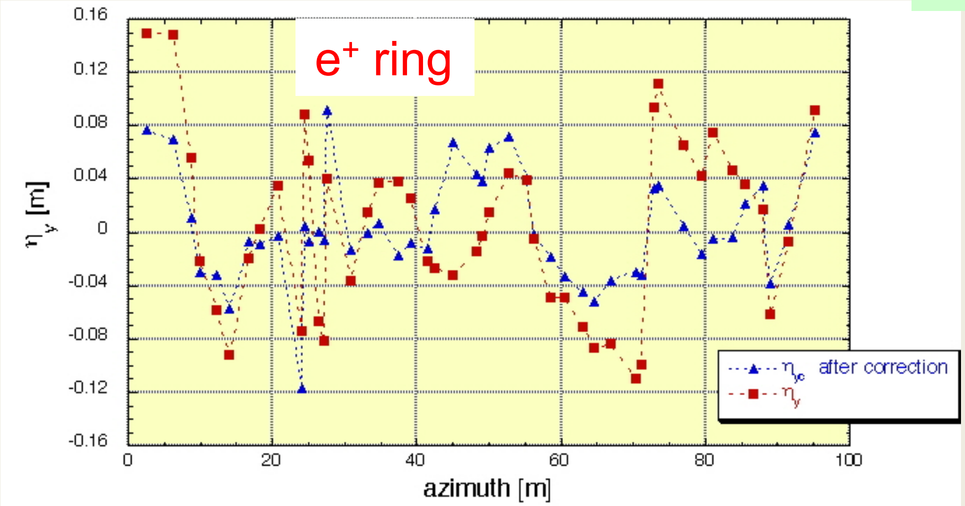

$(\eta_y)_{rsm} = 0.0647$ m

$(\eta_{yc})_{rsm} = 0.0411$ m

$\Delta(\eta_y)_{rsm} = -36\%$

$R^+ = 0.093$

$R^+_{\eta c} = 0.081$ measured @ SLM

$\Delta R^+ = -13\%$

Vertical Dispersion control & Main rings tuning

Closed Orbit Correction and steering magnet strength minimization help in:

- Finding errors in the magnetic layout
- Reducing the effect of non-linear contributions to the beam optics

Sextupoles alignment to avoid unexpected contribution to linear optics

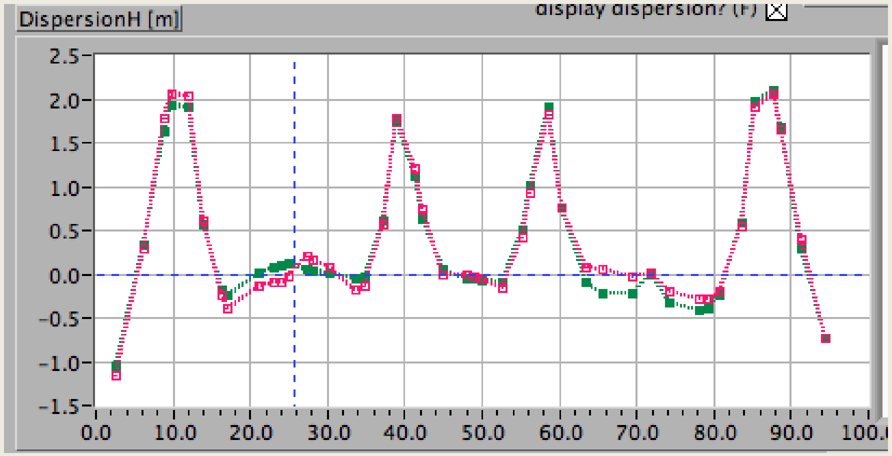

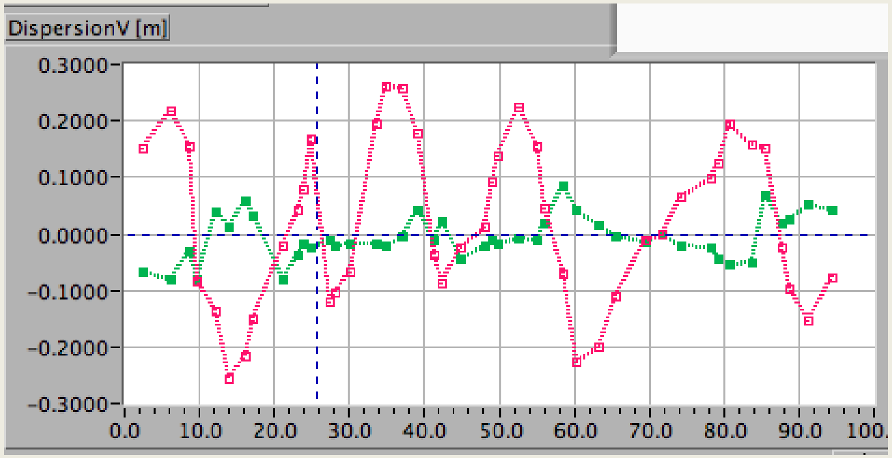

Dispersion evolution before (red MRp_29_11_2010) and after (green MRp_23_5_2011) closed orbit optimization and sextupole alignment

Wiggler measurement

The non-linear components of the WIGEL101 field are evaluated by measuring the beam tune shift dependence on the horizontal displacement bump at its place after switching off the sextupoles in that sector

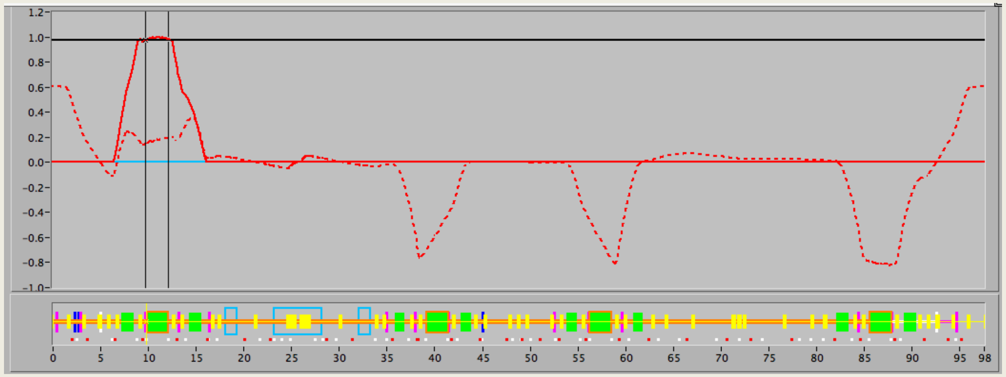

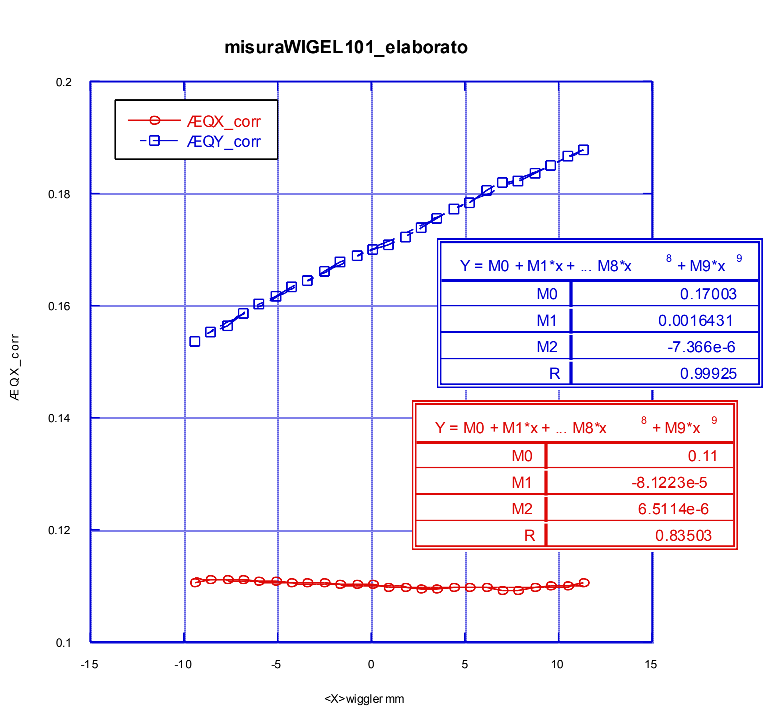

- $\Delta\nu_x$ and $\Delta\nu_y$ exhibit an evident linear behaviour excluding the presence of any octupole-like or higher component in the magnetic field
- A small sextupole-like dependence is observed in $\Delta\nu_y$ only, probably originated in the nearby dipoles included in the bump

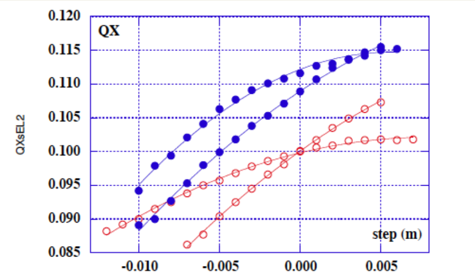

Figure 8: Measured horizontal betatron tune versus beam displacement in 4 wigglers

Published in 2004

K^3 [m^{-3}]	Year
800	2001
360	2004
0	2011

κ correction @ DAΦNE

FINUDA IR

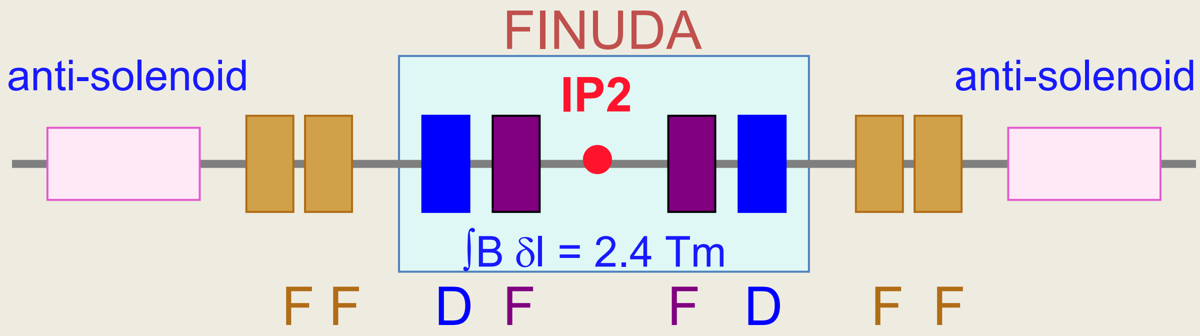

- ∫B δl = 2.4 Tm
- 2 superconductive compensator solenoids •
- 4 permanent magnet QUADs • •
- 4 electromagnetic QUADs •
- Independent QUADs rotation

- KLOE solenoids off (IP_1)
- $\varepsilon_x = .34\ \mu$

  $\Delta x \sim 13\ \sigma_x$ @ 1st par. cros.

  100 consecutive bunches (1 bucket 2.7 ns)
- low-β @ FINUDA IP_2

$\beta^*_x = 2.33$ m

$\beta^*_y = .024$ m

$\theta_x = .021$ rad

The main part of residual transverse coupling has been corrected by rotating the QUADs in IR2

Fine tuning is performed using skew QUADs

Betatron coupling correction

- local correction
  - by minimizing the coupling term of the measured Response Matrix by the IRs QUAD rotations $\Delta\phi_j$ j=1..8

$$M \Delta \phi = C^{meas}$$

$$M^{mod} = \begin{pmatrix} \frac{\partial y_{m_1}}{\partial k_{h1} \partial \phi_1} & \cdot\ \cdot\ \cdot & \frac{\partial y_{m_1}}{\partial k_{h1} \partial \phi_8} \\ \cdot & \cdot\ \cdot\ \cdot & \cdot \\ \cdot & \cdot\ \cdot\ \cdot & \cdot \\ \frac{\partial y_{m_{nBPM}}}{\partial k_{h\, n\, kick} \partial \phi_1} & \cdot\ \cdot & \frac{\partial y_{m_{nBPM}}}{\partial k_{h\, n\, kick} \partial \phi_8} \\ \frac{\partial x_{m_1}}{\partial k_{v1} \partial \phi_1} & & \frac{\partial x_{m_1}}{\partial k_{v1} \partial \phi_8} \\ \cdot & & \cdot \\ \cdot & & \cdot \\ \frac{\partial x_{m_{nBPM}}}{\partial k_{v\, n\, kick} \partial \phi_1} & & \frac{\partial x_{m_{nBPM}}}{\partial k_{v\, n\, kick} \partial \phi_1} \end{pmatrix} \qquad C^{meas} = \begin{pmatrix} \frac{\partial y_{m_1}}{\partial k_{h_1}} \\ \cdot \\ \cdot \\ \frac{\partial y_{m_{nBPM}}}{\partial k_{h\, n_{nkick}}} \\ \frac{\partial x_{m_1}}{\partial k_{v_1}} \\ \cdot \\ \cdot \\ \frac{\partial x_{m_{nmon}}}{\partial k_{vn_{kick}}} \end{pmatrix}$$

- linear system solved by SVD
- after few iteration 40% reduction in rms (C^{meas})

- global correction by SKEW QUADs

σ_y (KEK) = .3 mm

σ_y (PEP) > .4 mm

κ = .3%

measured by

- beam - beam scan
- beam aspect ratio @ SLM

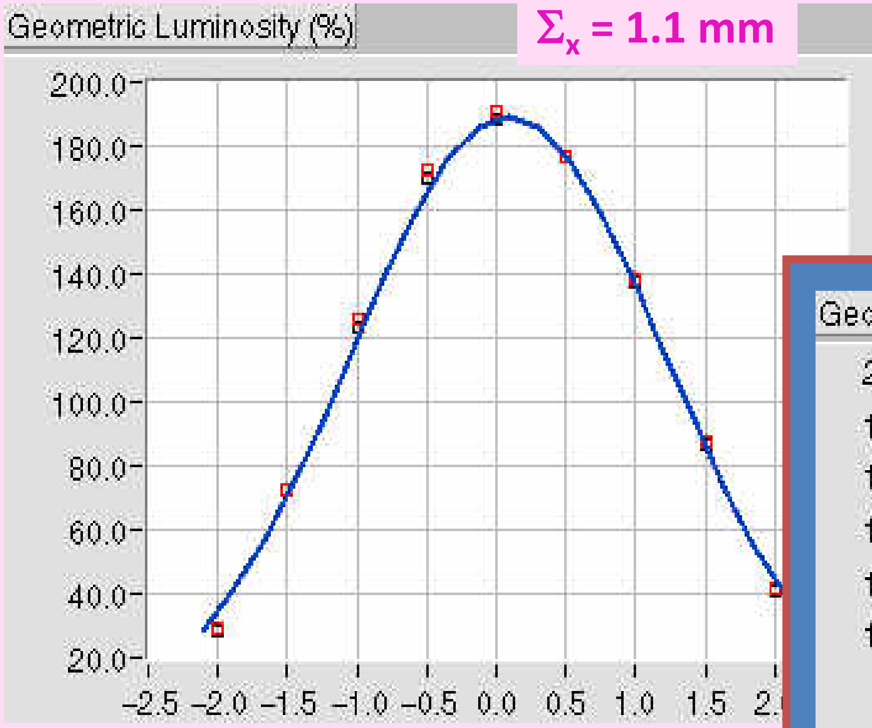

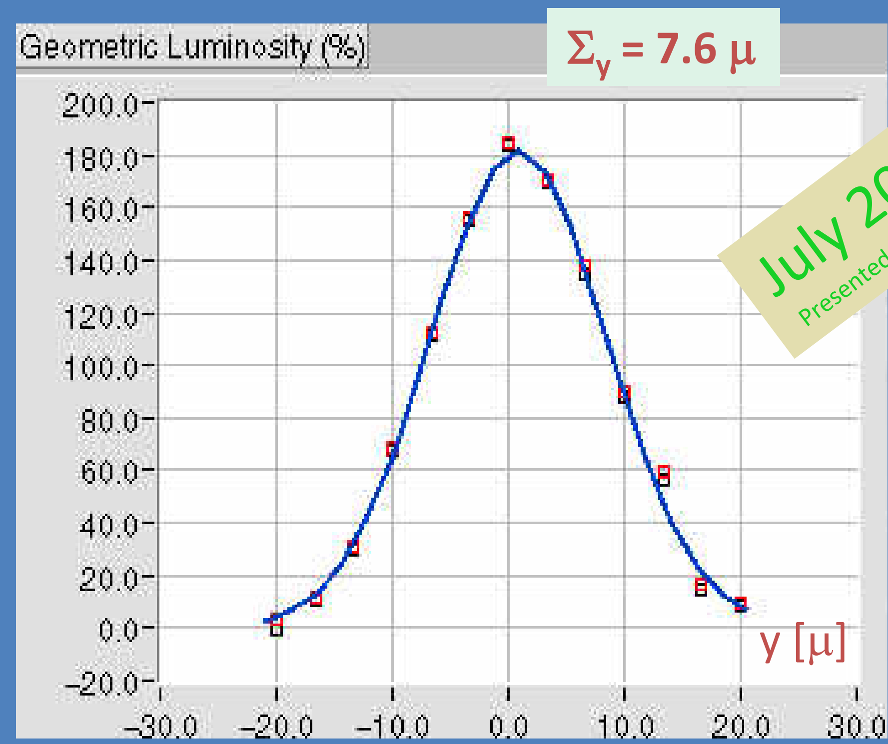

July 2006
Presented at EPAC04

$$\Sigma_{x,y} = \sqrt{(\sigma_{x,y}^{+\,2} + \sigma_{x,y}^{-\,2})}$$

The new KLOE-2 IR with the *Crab-Waist* collision scheme

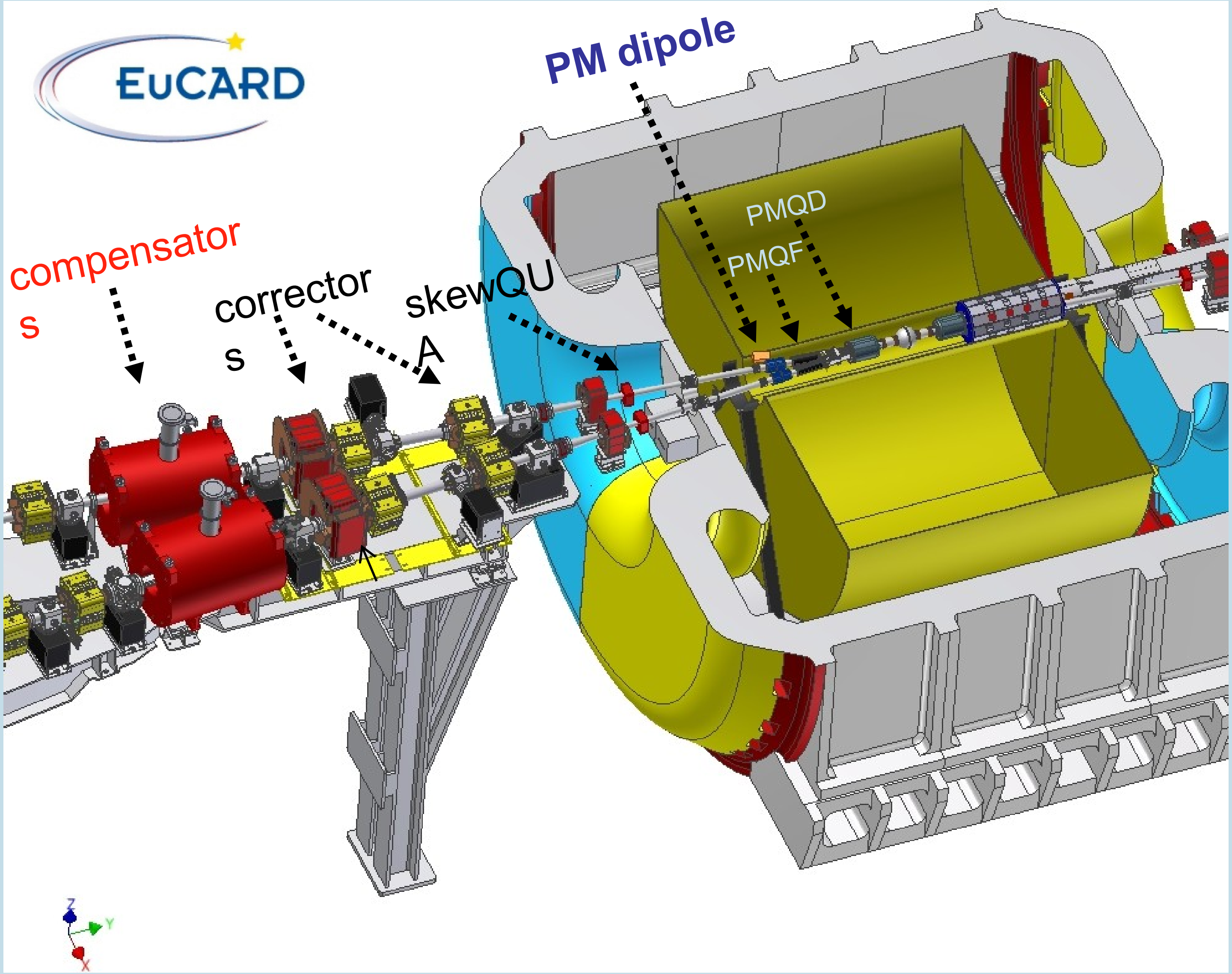

Coupling correction

•$\int_{KLOE} B \cdot dl$ canceled by 2 anti-solenoids for each beam

$$\int_{KLOE} B \cdot dl = 2.048 \quad [Tm] \quad \rightarrow \quad I_{KLOE} = 2300.[A]$$

$$\int_{comp} B \cdot dl = \pm 1.024 \quad [Tm] \quad \rightarrow \quad I_{comp} = 86.7[A]$$

To achieve coupling compensation also for off-energy particles

	Z from the IP [m]	Quadrupole rotation angles [deg] *Anti-solenoid current [A]*
PMQDI101	0.415	0.0
PMQFPS01	0.963	-4.48
QSKPS100	2.634	used for fine tuning
QUAPS101	4.438	-13.73
QUAPS102	8.219	0.906
QUAPS103	8.981	-0.906
COMPS001	*6.963*	*72.48 (optimal value 86.7)*

Fixed QUAD rotations

K is expected to be lower than for KLOE past

$K_{KLOE1} = 0.2 \div 0.3$ %

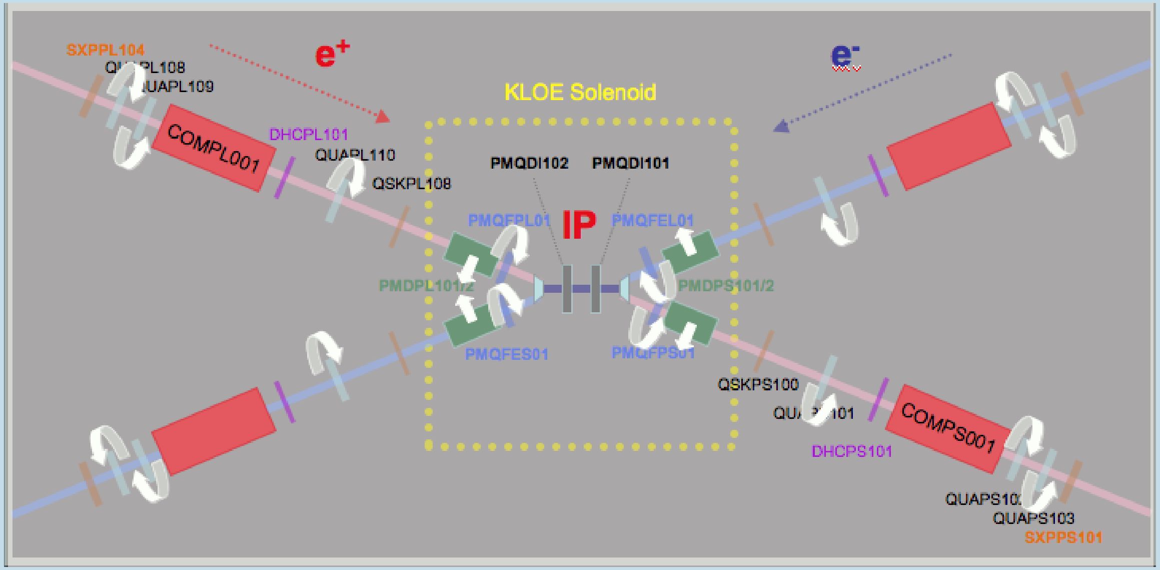

Betatron coupling analysis

- Transverse beam dynamics in presence of coupling is described by two normal modes
- normal modes when projected on the x-y plane are represented by an ellipse with a given eccentricity and tilt
- In this graphs the normal mode tilts computed from the ring model are compared with the corresponding values obtained from the measured steering magnet response matrices

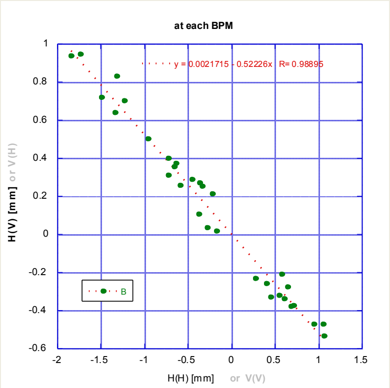

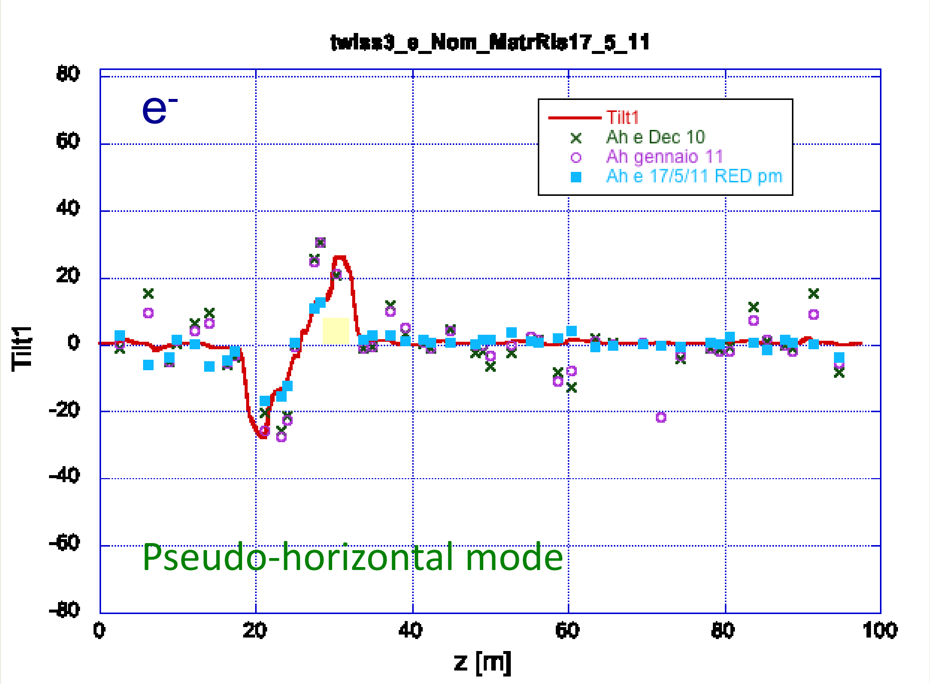

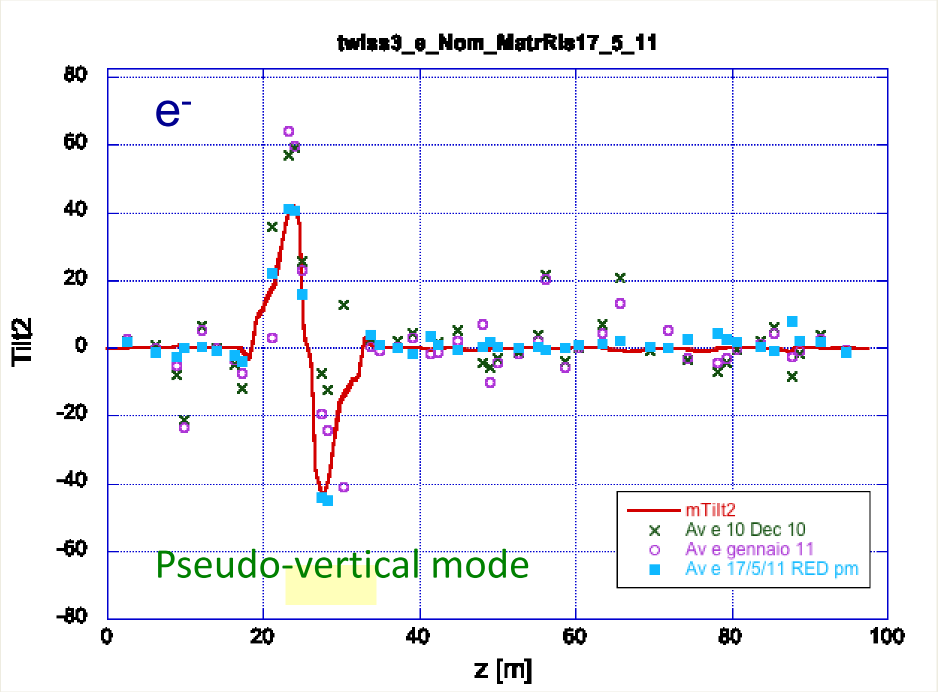

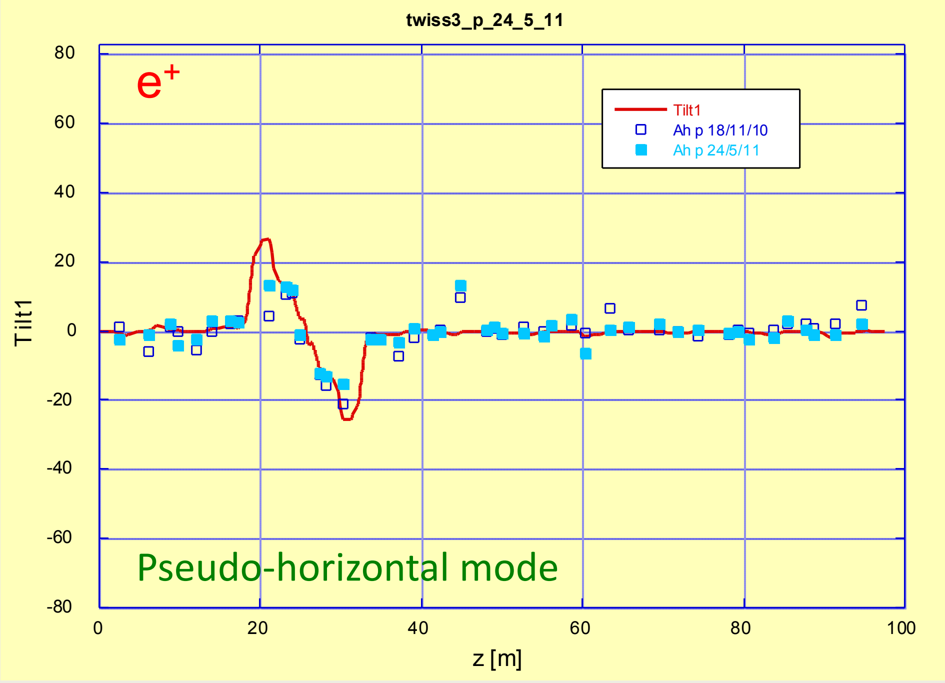
twiss3_p_24_5_11
e+
Tilt1
Ah p 18/11/10
Ah p 24/5/11
Tilt1
z [m]
Pseudo-horizontal mode

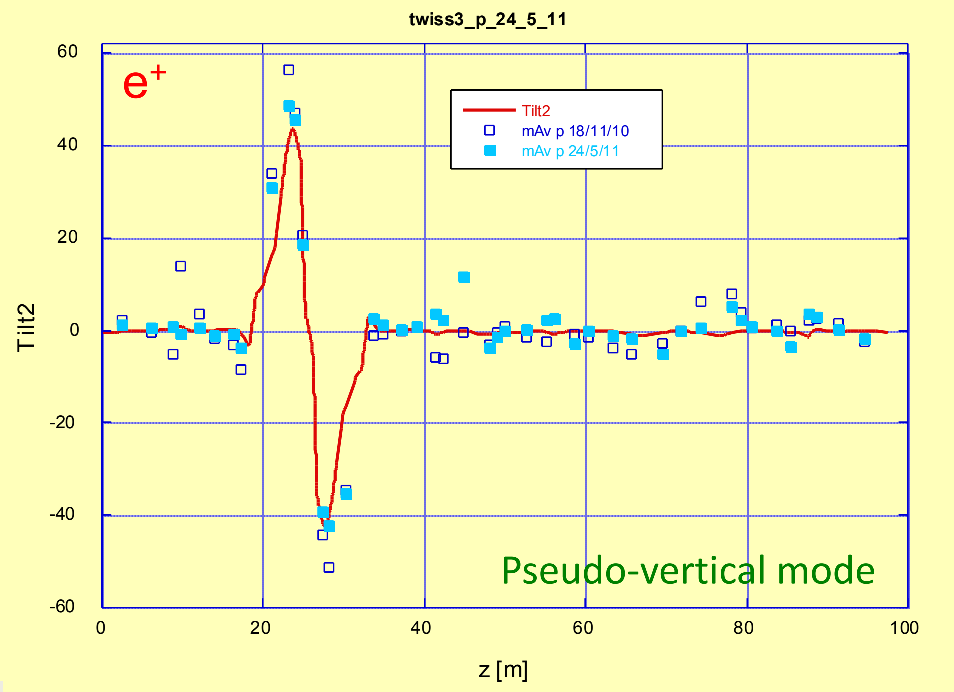
twiss3_p_24_5_11
e+
Tilt2
mAv p 18/11/10
mAv p 24/5/11
Tilt2
z [m]
Pseudo-vertical mode

Vertical beam-beam *Luminosity scan*

$$\Sigma_y = \sqrt{\sigma_{yp}^2 + \sigma_{ye}^2} \qquad \Sigma_y = \Sigma_y^{meas} * 0.88$$

May 2011

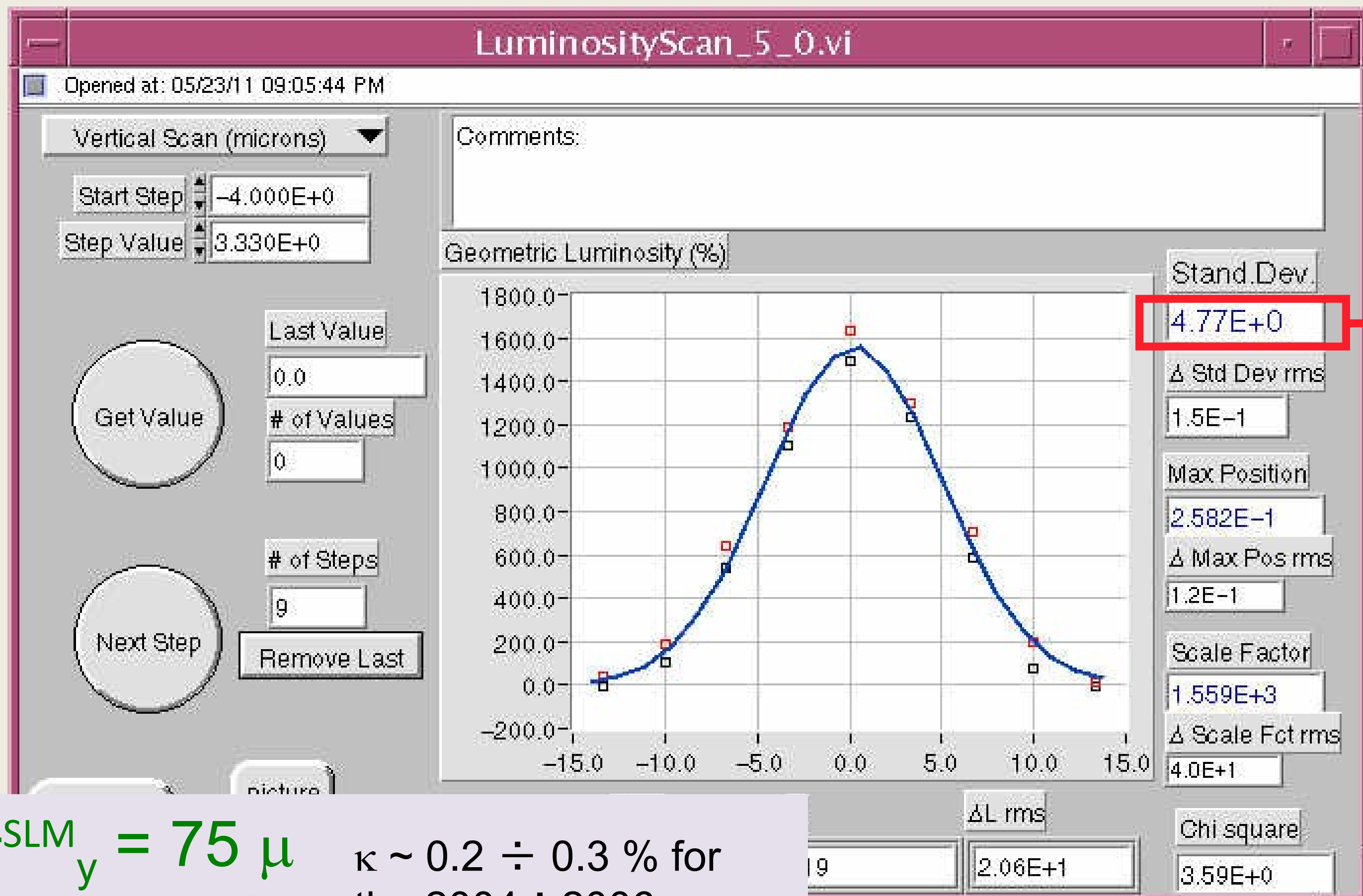

$\sigma_y \approx 3.0\,\mu m$

$\sigma^{SLM}_y = 75\ \mu$

$\kappa \sim 0.14\%$

$\kappa \sim 0.2 \div 0.3$ % for the 2004÷2006 KLOE run

Vertical beam-beam *Luminosity scan* *(SIDDHARTA run)*

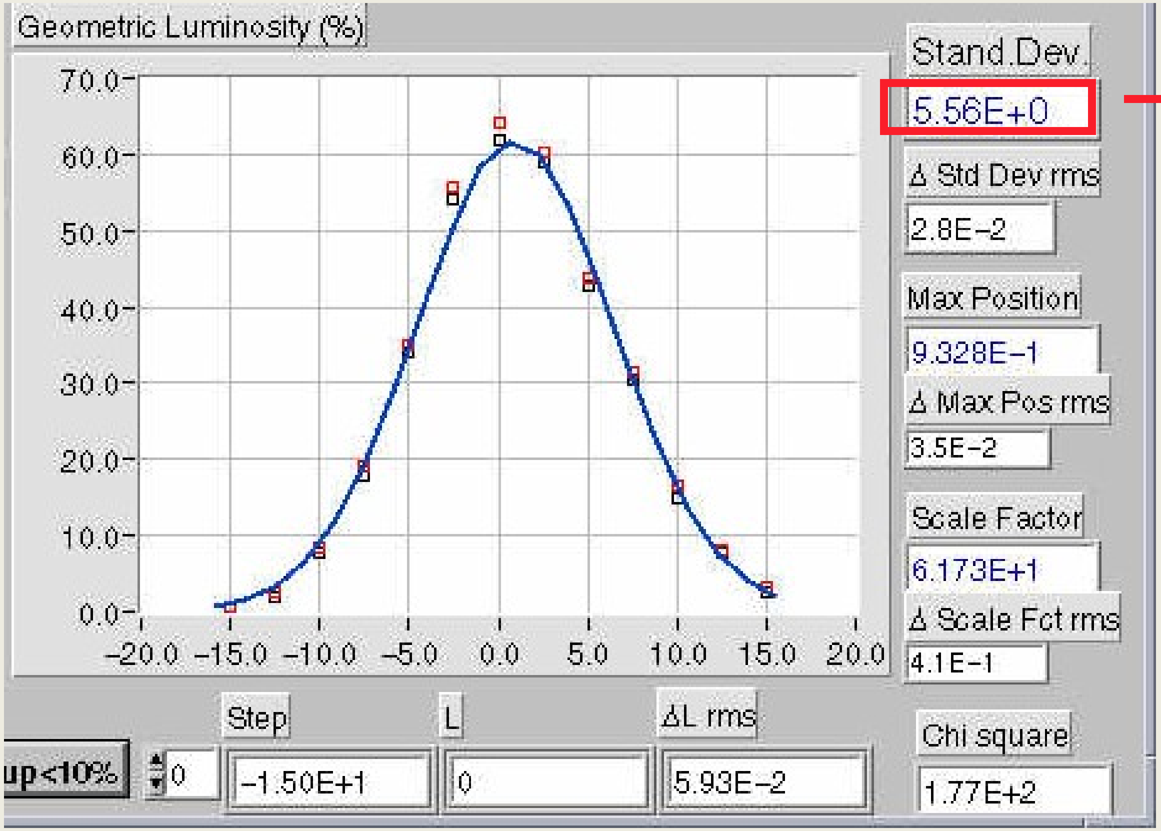

$\sigma_y \approx 3.5\mu m$

Design value 3.1μm

July 1st 2008

Presented PAC09

SIDDHARTA was a small detector without solenoidal field !!

Conclusions

The DAΦNE model has been essential in:

Setting up Collisions with:

- Two low-beta
- Low-beta in 1 IR and detuning the second one
- FINUDA
- DEAR
- KLOE

SIDDHARTA
KLOE-2 — *Crab-Waist* collision scheme

KLOE-2 with the solenoidal detector off

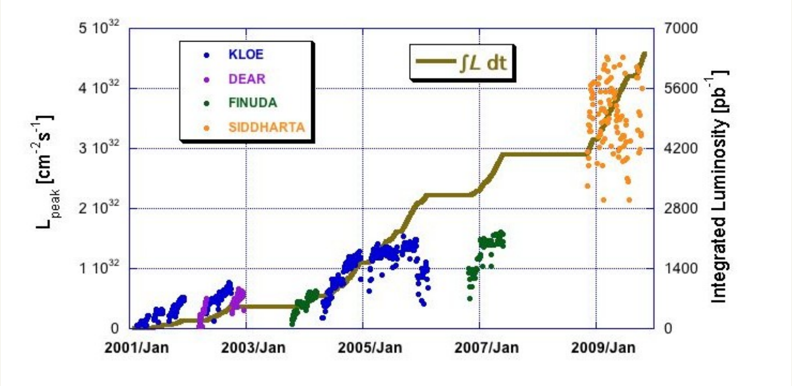

computing several optics configuration

- Detuning alternatively one of the two IRs
- Changing beam emittance
- Tuning crossing angle and β in the IR
- High momentum compaction
- Negative momentum compaction

The model has been extensively used to investigate recognize and mitigate several limiting factors affecting the collider performances.
All those studies paved the way to the many progressive upgrades implemented on DAFNE during the past years

Acknowledgment

I like to thank: A. Stella, A. Drago, M. Preger, P. Raimondi, D. Alesini, M. Zobov